Towards Fish Individuality-Based Aquaculture

Rudolf Schraml, Heinz Hofbauer, Ehsaneddin Jalilian, Dinara Bekkozhayeva, Mohammadmehdi Saberioon, Petr Cisar, and Andreas Uhl

***Abstract*—By bringing concepts of precision farming to intensive aquaculture fish production, it can be optimized to be more sustainable while focusing on fish welfare criteria. This requires a shift from mass to smart production and to consider each fish as an individual. Therefore, it is required to be able to identify each fish in a tank or sea cage. In this article, we prove the feasibility of fish identification using the iris as a biometric characteristic. Based on a new dataset, captured in a controlled out of water environment: 1) a fully automated iris recognition system is presented and utilized for the experiments and 2) the distinctiveness and the stability of the iris pattern of Atlantic salmon (*Salmo salar*) is assessed. Results prove the distinctiveness, which indicates that the iris pattern of Atlantic salmon is suited for biometric identification. However, the iris pattern has a low stability, which means it changes over time. Due to frequent interaction of fish and system, usually multiple times a day during feeding, there is ample opportunity to keep the biometric template up-to-date, which makes the lack of long-term stability a nonissue. It can be concluded that a biometric fish identification system is feasible, with the precondition that biometric templates of each fish are periodically updated to combat the low stability.**

***Index Terms*—Fish iris identification, precision fish farming (PFF).**

I. Introduction

THE PRODUCTION requirement of aquaculture in the last 30 years has risen steeply and continues to do so. The edible fish consumption per capita is rising and outpaces the naturally occurring fish population, making this consumption sustainable only through aquaculture production. This trend will not decline and aquaculture production plays a crucial role to ensure sustainable development in economic, social, and environmental terms [1].

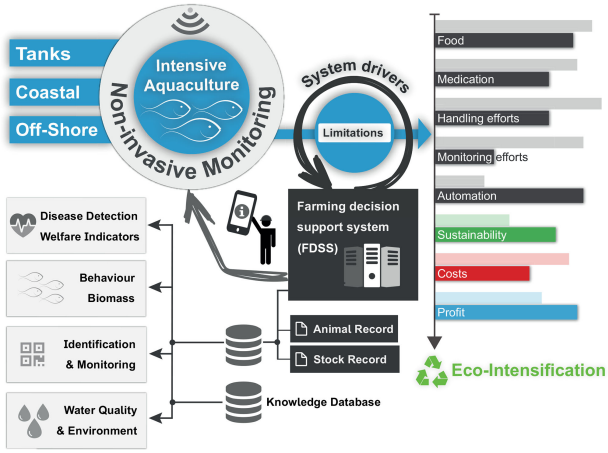

Fig. 1. Farming descision support system (FDSS).

For intensive aquaculture, the fish is cultivated in tanks or sea cages. An increase in production can often only be achieved through a higher density of fish. This exacerbates problems in the management of disease and health of the fish. Optimization of fish production, therefore, also requires an improvement of fish welfare. Toward precision fish farming (PFF) control-engineering principles are applied to fish production, thereby improving the farmer's ability to monitor, control, and document biological processes [2]. The move from mass to smart production allows application of control-engineering principles to individual fish instead of the population as a whole. It is all about data, which are collected, analyzed, and exchanged almost in real time, allowing for medication or removal of individual fish as well as the optimization of yield per fish. Smart production requires that data are assigned or linked to a set of objects or single (living) objects in the production. Data and information enable to improve and/or completely rethink well-established processes.

Further, regarding intensive aquaculture considering each fish as an individual, requires noninvasive monitoring to set up a farming decision support system (FDSS). *This type of* smart fish farming as envisioned by a FDSS relies on the identification of individual fish. Fig. 1 illustrates our vision for such a system that follows the paradigm of ecological intensification. This system enables to assign information about fish traits such length, weight, sex and maturity, and fish skin color during different growth stages to the corresponding animal or stock record, to monitor growth status for better management [3]. Common ways for individual identification of fish are invasive

Manuscript received March 5, 2020; revised June 3, 2020; accepted June 24, 2020. Date of publication July 3, 2020; date of current version March 5, 2021. This work was supported in part by the Austrian Science Fund (FWF) under Project I 3653 in part by the AquaExcel2020 TNA Project AE050006, in part by the European Unions Horizon 2020 research and innovation program under grant agreement No. 652831 (Aquaexcel2020 – TNA Project AE05006), and in part by the Ministry of Education, Youth and Sports of the Czech Republic – project CENAKVA (LM2018099). Paper no. TII-20-1159. *(Corresponding author: Rudolf Schraml.)*

Rudolf Schraml, Heinz Hofbauer, Ehsaneddin Jalilian, and Andreas Uhl are with the Department of Computer Sciences, University of Salzburg, 5020 Salzburg, Austria (e-mail: rudi.schraml@gmail.com; hhofbaue@cosy.sbg.ac.at; ejalilian@cs.sbg.ac.at; uhl@cosy.sbg.ac.at).

Dinara Bekkozhayeva, Mohammadmehdi Saberioon, and Petr Cisar are with the Institute of Complex Systems, University of South Bohemia in České Budějovice, 370 05 České Budějovice, Czechia (e-mail: dbekkozhayeva@frov.jcu.cz; msaberioon@frov.jcu.cz; cisar@frov.jcu.cz).

Color versions of one or more of the figures in this article are available online at https://ieeexplore.ieee.org.

Digital Object Identifier 10.1109/TII.2020.3006933

methods relying on tagging and marking [4]. Invasive methods may cause technical as well as health and animal behavioral problems amplifying a problem we want to solve. Even currently available noninvasive approaches (e.g., external colorants) may cause behavioral alteration and pose health risks, which require to take care of welfare issues [5]. Furthermore, invasive identification is time consuming and incurs a substantial cost. *To avoid these problems* and additional cost, it would be optimal to be able to have a noninvasive and contact free identification method.

For this article, and the envisioned FDSS, the focus is on noninvasive fish identification using biometric characteristics of the fish body. Specifically, we will evaluate the suitability of the iris for this purpose, since it is always visible (due to lack of eyelids), permanent (as opposed to skin patterns e.g., [6]) and has a good track record for humans and other animals (e.g., for cow identification [7]).

The rest of this article is organized as follows. First, in Section II, a review on related work is presented, followed by the main contributions of this article. Section III introduces the computation and matching of fish iris codes (FICs). The experimental setup and evaluation are presented in Section IV, and finally, Section V concludes this article.

II. Related Work and Contributions

Literature on fish identification can be categorized based on 1) the direction from which the fish and the biometric characteristic is captured: lateral, dorsal, or ventral and 2) based on the utilized feature extraction/matching approach, e.g., skin pattern or shape features. Although there exists plenty of research, only a few approaches make use of machine vision methods.

In the works of [8]–[10], the identification of different fish species was examined on the basis of lateral images. The regions, utilized for biometric feature extraction, were selected manually. For Patagonia catfish identification in [8] skin pattern spots were marked manually (position and size) and three reference points set the region of interest (ROI). For 45 fish, which were captured 14 times for 254 days, a Rank-1 identification accuracy of 96% was reported. Similarly, for Atlantic salmon identification in [9] spots were marked manually and utilized for a specific matching algorithm, requiring at least three spots. At the age of 12 months most fish showed less than three spots and 17 out of the 20 remaining fish were identified correctly. For lionfish identification in [10], three different ROIs were selected in which speeded up robust features (SURF) keypoints are detected, computed, and used for matching. For the best body part (flank) and 48 individuals, captured at one point in time, the authors report a Rank-1 identification accuracy of 68%.

In [11], [12] dorsal head view images were assessed as biometric characteristic. For Chinook salmon identification in [11], the ROI was marked manually, the spot pattern was binarized and the spot centroid coordinates were used as biometric features. Results show 100% identification accuracy for fish that developed a pattern, which was only the case for 42% of all fish (=295 fish captured seven times over 251 days). Castillo *et al.* [12] used a reverse image search engine to assess delta smelt identification based on three manually selected ROIs. Fish were captured at three points in time and for the fusion of the two best areas, an identification rate of 94% for adjacent sessions and 59.2% between the first and the last session was reported.

In [5], naked-eye and computer-assisted identification of armored catfish based on ventral images, captured in laboratory and field conditions, were evaluated. The computer-assisted approach is based on scale invariant feature transform key points. ROIs were selected manually and results for 120 comparisons from the laboratory and 224 comparisons from the field data showed an identification accuracy (Rank-1) of 82.2% and 93.8%, respectively. These prior works have following two major shortcomings.

1) Manual annotation of the ROI and/or the utilized biometric information/pattern is required. Such an approach is well-suited for small-scale experiments, but it is not applicable on a large scale, i.e., for intensive aquaculture and the envisioned FDSS. For example, Dala-Corte *et al.* [5] reported that for 225 comparisons, 17 min were required for computer assisted identification.
2) Related literature has shown that the skin pattern is not universal; some fish do not form them and are not stable once formed. That is, the assessed skin patterns change over time and some fish showed no pattern at all or only formed them at some later stage of growth. This can even vary for minimal divergence from a base strain of fish; for example, [6] showed that some Zebrafish mutations show no more pattern at all.

Regarding these shortcomings, we will look at iris patterns in Atlantic salmon as member of the Salmonidae family. All members of this family have eyes and are lidless, making the iris a universal trait. The basic layout of the iris biometric toolchain known from human iris biometric identification will be used (and be described later). While this solution sounds reasonable, the following has been evaluated in order to see if the iris is a usable biometric characteristic.

1) *Localization and Orientation of the Iris:* To establish fully automated fish identification, it is required to detect the iris region automatically and to rotationally prealign each iris preliminary to feature extraction and matching. Hence, for the Atlantic salmon iris, a segmentation approach is introduced, and a set of rotational prealignment strategies is tested.
2) *Stability:* The lifespan of an intensive aquaculture fish is short, but the fish grows rapidly within this timespan. Thus, another contribution of this article is to evaluate the stability of the Atlantic salmon iris pattern, i.e., if and how the pattern changes over time.
3) *Automatic Iris Recognition System:* In contrast to other works in this field, the evaluation is done using state-of-the-art biometric system evaluation protocols and metrics. Regarding fish iris image processing and biometric identification a fully automated system will be assessed.
4) *R^3 Research Principles:* Replicability, Reproducibility and Reusability. In order to repeat, improve or develop new methods for fish iris biometry a database is required. Thus, we make public the acquired database of fish iris images (see Section IV-A) including source code and libraries at a GitHub repository.[1]

[1][Online]. Available: https://github.com/rschraml/fishid

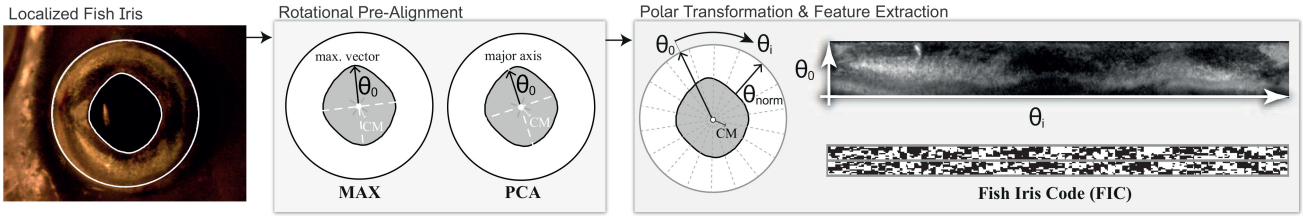

Fig. 2. Illustration of the pipeline to generate the fish iris code (FIC) from a segmented image.

To sum up: Our contribution is a state-of-the-art based fish iris identification system based on a universal trait. However, we note that the main objective of this article is to assesses the basic feasibility of such a system and that the experimental evaluation is based on fish iris images acquired in a controlled out of water environment.

III. Fish Iris Codes

The first step in the biometric toolchain is to acquire an iris image for which a fish iris code (FIC) is computed in four consecutive steps (see Fig. 2): iris segmentation, rotational prealignment, iris normalization, and feature extraction.

A. Fish Iris Anatomy

The anatomy of fish eyes is similar to the human eye anatomy on a basic level. Considering the human eye, we are looking at the stroma, a fibrovascular layer connecting the sphincter (for closing the iris) and dilation (for opening the iris) muscles or the eye. The layer consists of fibers (fibro-), some running in a circular pattern, but mostly radially mixed with nerves and blood vessels (-vascular). In addition to the fibres, the dilation muscle also runs along the radial axis. The formation of the fibres in the stroma is different for individuals and stable over time, which makes it a perfect candidate for biometric recognition of humans. If the stroma contains pigments, it appears dark and the structures are not apparently visible. To counteract this, the human iris is captured with near-infrared cameras where the pigmentation does not interfere with image acquisition.

For fish there are differences pertaining the iris, which are not uniform over classes of fish. Iris of different fish species can differ in terms of muscle, shape, and function, which leads to a noncircular iris pattern, for example. As such the usability of the iris for fish identification has to be judged for different fish classes and species. For salmon, the iris is nonfunctional in that it does not open or close to moderate light, i.e., it does not exhibit a photometric response. Instead, the salmon uses retinomotor movement of photoreceptors and retinal pigmentation to change the light exposure of rods and cones [13], [14]. The iris is well-formed and prominent despite its vestigial function. It is an extension of the epithelial pigment layer of the retina (which is used to moderate illumination) [15]. The pupillary opening shows rounded diamonds shape (see Fig. 2).

B. Fish Iris Segmentation

For iris recognition the pupillary boundary, i.e., between pupil and iris, and the limbic boundary, i.e., between iris and sclera (the white of the eye in humans), need to be detected. This allows 1) to segment the ROI containing the biometric information and 2) to polar transform this ROI to an uniform rectangular representation. Traditional human iris segmentation approaches are not well-suited as they often rely on the circular shape of the human iris. For example, we mention the segmentation approaches contrast-adjusted Hough transform (CAHT) [16] and weighted adaptive Hough and ellipsopolar transform (WAHT) [17]. Preliminary experiments using a traditional morphological-based segmentation approach led to poor results, which are not worth to be considered. However, recent research showed segmentation approaches based on convolutional neural networks (CNN), which are well-suited for human iris segmentation. For instance Hofbauer *et al.* [18] showed that a CNN-based semantic segmentation approach outperforms traditional approaches like CAHT in case of low quality databases. Based on this insight, the inapplicability of traditional iris segmentation methods and the insufficient results with the tested morphological approach a CNN-based semantic segmentation approach, requiring groundtruth data, has been envisioned. Thus, for all images in the utilized database the pupil (=inner boundaries shown in Fig. 3) was detected in a semiautomated manner. The black pixels of the pupil where clustered, holes where filled and the boundaries were corrected manually to avoid under/over segmentation. The limbic boundary (=outer boundary) was approximated based on the pupillary boundary. Basically, by a circle the center of which is defined as the pupil center of mass (CM). The radius is 2× larger as the mean distance between the CM to pupillary boundary vector lengths. The semiautomated estimated pupillary boundary and approximated limbic boundary are supposed to bound the groundtruth for the iris.

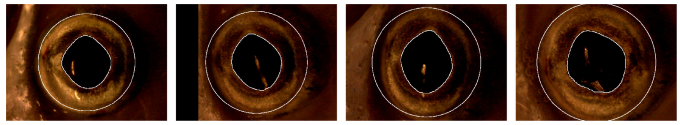

Fig. 3. CNN-based segmentation results for fish #0F571E captured in four time delayed sessions. As shown, the iris is growing significantly from Session 1 to 4, accompanied by changes in the iris pattern.

CNNs are a multilayered class of artificial neural networks that gained great success in resolving many key computer vision challenges such as visual segmentation. The network architecture we used to segment the fish pupil is identical to the "SegNet-Basic" fully convolutional encoder–decoder network [19]. The network's encoder architecture is organized in four stocks, containing a set of blocks. Each block comprises a convolutional layer, a batch normalization layer, a ReLu layer,

and a pool layer with kernel size of 2×2 and stride 2. The corresponding decoder architecture, likewise, is organized in four stocks of blocks, whose layers are similar to those of the encoder blocks, except that here each block includes an up-sampling layer. The decoder network ends up to a soft-max layer, which generates the final segmentation map. The network implementation is realized in the Caffe deep-learning framework. As ground-truth data the semiautomated segmented pupils were utilized. In order to perform, the segmentation on all available images in the database and yet keep the training and testing separate, we used the twofold training scheme. In particular, we divided the whole database into two equal parts, and used one part as our testing data and the other one as our training data. Then, we switched the training and testing folds, and so we obtained the pupillary boundary for each iris image in the database. The limbic boundary was approximated in the same way as for the semiautomated segmentation. Exemplary results are shown in Fig. 3.

C. Rotational Prealignment and Polar Transformation

During matching of two FICs rotation compensation can be performed by comparing shifted versions of the FICs. However, the available fish iris data shows exceptionally strong rotational differences between images of the same iris (see Fig. 3). Compensating for such large angular differences is too slow. The goal of rotational prealignment preliminary to feature extraction is to reduce the rotational differences to an extent where they can be compensated in the matching phase without undue loss of speed. For this article two different prealignment strategies (PCA, MAX) have been implemented which are assessed in the experimental evaluation (see Fig. 2). Both strategies rely on the observation that the fish pupil is not circular and thus it is assumed that a prealignment vector (Θ_0) can be determined. For the first strategy, principal component analysis (PCA) is applied to the points of the pupillary area, which leads to two perpendicular eigenvectors giving the major axes of the pupillary. The dominant axis is then used as prealignment vector. For MAX the pupillary boundary is first smoothed with a Gaussian filter and the vector with the maximum CM to pupillary boundary distance is utilized as prealignment vector (Θ_0). In the experiments, it was observed that for both approaches it happens that for iris images captured at different dates the prealignment can lead to 90° flipped versions.

D. Normalized Polar Transformation

Features are extracted from a normalized iris texture. Note that no image enhancement has been applied to the iris texture. The iris is polar transformed using Daugman's rubber-sheet model [20], this is in essence an unrolling of the iris texture, and stretching to a uniform size. This normalization corrects two factors which can lead to a different iris texture area: 1) The distance and angle between the camera and iris can vary, which introduced a scale change and geometric distortion; and 2) as the fish grows, so does the skeletal and soft tissue, including the eye. The polar transformation on the other hand allows for a rotation of the eye to be expressed as a horizontal shift, which is much easier to compute. Such a rotation can happen due to a rotation of the fish in the water or of the eyeball in the eye-socket. For our normalized polar transformation, Θ_0 (calculated in prior steps) is used as initial vector used to unroll the iris into the polar domain which is positioned on the left edge of the transformed fish iris (see Fig. 2). For normalization each pixel in the polar image is stretched according to the length of Θ_{norm}, which is specified as the largest pupillary to limbic boundary vector. For the transformation bicubic interpolation is applied.

E. Feature Extraction

For feature extraction and matching of FICs, we use the open University of Salzburg Iris Toolkit (USIT) [21]. A note on transfer learning and domain specific improvement: To transfer knowledge from one domain (human iris) to another (fish iris), we simply used the USIT methods as is to see what does work and what does not. Specifically, the one-dimensional (1-D)-Log-Gabor [16] based feature extraction worked very well and we kept that as is, the segmentation on the other hand did not work at all, mostly due to a difference in the shape of the iris and periocular tissue, so most of our attempts to improve the knowledge transfer fell into this part (=feature extraction) and the polar transformation of the iris biometric toolchain.

1-D local Gabor features are extracted from a number of 1-D signals. To generate the 1-D signals from the texture, we first split the texture into horizontal bands with a height of roughly 8% of the distance from pupillary to limbic boundary. Then, the remaining verticality is removed by averaging the values for each horizontal position. This combination of information along the radial axis counteracts sampling artifacts due to resolution and different pupillary dilations. Since the outer boundary is only an approximation we will not use the outermost parts (about 20%) in the comparison since they might contain scleral or noneye textures. The Gabor filter used has a real and an imaginary component, which roughly equate to an edge (change in signal) and a line (constant signal) filter. This relates to radial edges and lines features in the unrolled image.

Note: To reduce the size of the FIC, we only use the signs of the line and edge filters, which represent the absence of lines and edges, respectively.

IV. Experiments and Results

A. Salmon Iris Image Database (SIIDB)

SIIDB was captured 2018 by the authors within the AquaExcel2020 TNA project AE050006, FISHID. SIIDB is hosted at https://github.com/rschraml/fishid. For image acquisition 330 adult Atlantic Salmon (∼1kg, 42–46 cm length) were selected initially. The cultivation period is usually between 12 to 18 months in tanks and between 12 to 24 months in sea cages. For iris image acquisition the USB microscope Dino-Lite AM3113T (no additional light) was utilized. A spacer [see Fig. 4(a)] was utilized to keep the distance, roughly constant. Each fish was anesthetized [see Fig. 4(b)] and one iris (head showing to the left) was captured several times (8–16×) with minor rotations caused by movements of the fish. Unusable images due to blur of focus problems were removed. The database is subdivided into a short-term (ST) and a long term (LT) dataset. A schematic

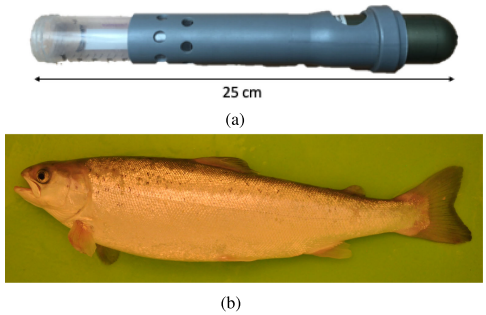

Fig. 4. SSIDB: Utilized sensor and exemplary lateral image of an Atlantic salmon fish from the LT dataset. (a) Dino-Lite AM3113T with spacer. (b) Fish with ID #0F571E –Session 1.

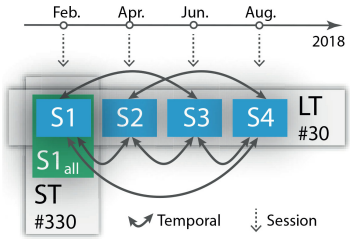

Fig. 5. Testset structure overview.

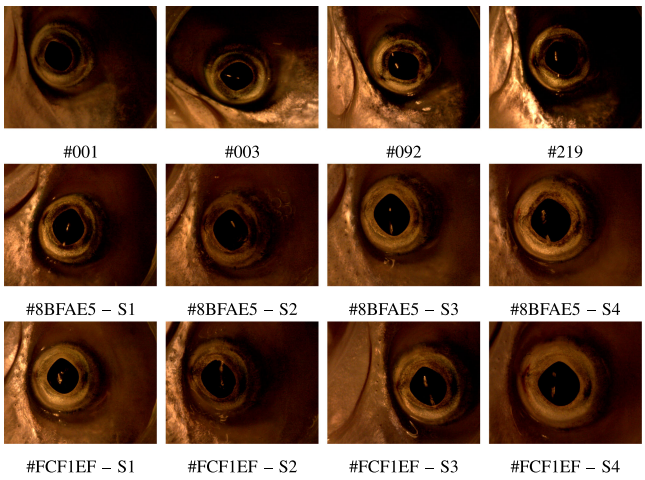

Fig. 6. Exemplary iris images of the ST (row 1) and LT dataset (row 2 and 3).

overview of the database structure is illustrated in Fig. 5. The ST dataset are composed of iris images from 330 different salmon fish, which were captured within one week. For the LT dataset, a subset consisting of 30 fish from Session 1 (S1) was captured again in three subsequent sessions (S2,S3,S4) with approximately two months time span in between. Exemplary iris images for four different fish of the ST dataset and two fish of the LT dataset are depicted in Fig. 6.

B. Experimental Setup

For all fish iris images in the LT and ST dataset FICs were computed for different rotational prealignment strategies, which results in a set of configurations (MAX, PCA, MAX_{OPT}, PCA_{OPT}) as described in Section III-C.

Furthermore, two additional configurations based on PCA and MAX were used, utilizing four FICs per iris image. One FIC is the same as for regular PCA and MAX and the other three have a 90°, 180°, and 270° rotational offset from the first. These configurations are denoted as PCA_{ROT} and MAX_{ROT}. The goal is to avoid errors caused due to 90° rotated versions of the same fish iris. During matching the best match (=highest similarity) between the four FICs of each iris is determined and used as matching score (MS). One baseline configuration (NO) is computed without applying rotational prealignment. All configurations were computed for semiautomated (GT) and CNN segmented (CNN) fish irides in SIIDB.

For each configuration and all combinations of FICs MSs are computed. MSs which are computed between FICs from the same session are denoted as session MSs and MSs computed between FICs from different sessions as temporal MSs (see Fig. 5). Session MSs are computed for the ST dataset together with the data of S1 from the LT dataset. The corresponding score distribution (SD) is denoted as S1_{all}. Furthermore, session MSs are computed for the different sessions of the LT dataset, which results in four different SDs denoted S1, S2, S3, and S4, respectively. Temporal MSs are computed between the different sessions of the LT dataset that leads to six different comparisons: S1↔S2, S2↔S3, S3↔S4, S1↔S3, S2↔S4, and S1↔S4. Note that each session and temporal SD is further subdivided into an intra and interclass SD, which correspond to the genuine and impostor SDs in biometrics [22]. Genuines are MSs computed between FICs from the same fish and impostor MSs are computed between FICs from different fish.

a) Fish Iris Distinctiveness and Stability: The results for ST and LT evaluations present an insight into the distinctiveness (same session performance) and stability (change over time) of the Atlantic salmon fish iris. Both are quality criteria of a biometric characteristic. Distinctiveness is the main prerequesite and expresses that the biometric characteristic enables the distinction between different individuals. Stability is crucial for the robustness of a biometric system and expresses that the biometric characteristic does not change or vary over time. Intrinsic changes mainly result from ageing. Extrinsic changes are caused by different acquisition conditions, e.g., light or position (rotation, tilt, and camera distance) of the fish.

In the following, we experimentally assess fish iris distinctiveness and stability. The session SDs enable to draw conclusions on the distinctiveness of the fish iris and the temporal SDs enable to assess fish iris stability. Furthermore, results for semiautomated and CNN-based segmentation enable to draw conclusions on the theoretical performance, as well as for a fully automated biometric system.

C. Results and Discussion

The experimental evaluation is done in four steps. 1) It is assessed how much rotation is in the data. Since rotation negatively influences the MSs we need to ascertain if rotational prealignment is required or if rotation compensation in the

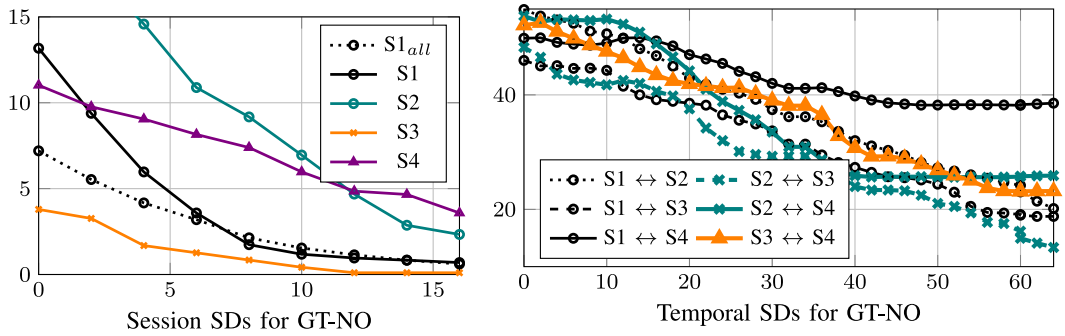

Fig. 7. EERs for different rotation compensation shifting values [*X*-axis: Rotation compensation in ±Bit, *Y*-Axis: EER in %].

matching stage is sufficient (Section IV-C1). Thus, rotational differences in the session and temporal SDs are assessed by comparing the results of the baseline configurations where no rotational prealignment (NO) is applied. 2) We assess the basic suitability of the different rotational prealignment strategies by analyzing the verification performances for the temporal and session SDs (Section IV-C2). 3) Identification performance results are presented. Results for the temporal and session SDs reflect real world scenarios in terms of repeated identification with no time delay and varying time delays for tracking and monitoring of a fish (Section IV-C3). 4) Finally, the presented results are contrasted with the results presented in related literature.

1) Rotation Compensation Performance: In order to get an impression of the rotation, which is contained in the LT and ST dataset an analysis of the verification performances of NO for the session and temporal SDs is performed. For verification performance evaluation the equal error rate (EER) is a general benchmark. Basically, the question is if shifting during matching is sufficient to overcome rotational variations, i.e., to show the need for rotational prealignment. To avoid side affects caused by segmentation errors the semiautomated segmented fish irides (GT) were utilized.

It is expected that with an increasing shifting value the EER decreases until a lower boundary is reached. Therefore, the shifting value in the matching stage is varied from 0 to 16 for the session SDs and from 0 to 64 (stepsize 2) for the temporal SDs and it is assessed how the EERs change. A shifting value of 1 corresponds to a rotation of $360°/512 = 0.7°$, where 512 is the width of the polar transformed and normalized iris. This means that the maximum amount of rotation, in case of the temporal SDs, which has been compensated for is $+/- 44.8°$.

The charts in Fig. 7 show the EERs achieved for different shifting values and the different session- and temporal SDs, respectively. For the session SDs rotation compensation in the matching stage is sufficient to achieve good performances (EERs<4%) with a shifting value set to 16. Even with a lower shifting value of 8 EERs below 9% are achieved. However, rotation compensation is required to attain acceptable EERs for the temporal SDs. The difference between the session and temporal SDs can be attributed to the data acquisition. Within a session the rotational variation for the iris images of a fish were nominal and mainly caused by body movements of the fish. For each new acquisition session each fish was once again positioned on a table, which leads to stronger rotational differences in the temporal SDs. For the temporal SDs in the right chart of Fig. 7, it is obvious that this shift-based rotation compensation is not sufficient to overcome the rotational variations. Even with very high shifting values no acceptable EERs are achieved. Whereas for the session SDs a shifting value of 16 is suited to achieve EERs below 4%, for the temporal SDs all EERs stay over 39%. While it would be possible to use a higher shift-based rotation compensation this affects the outcome in terms of timeliness, i.e., matching would take longer, as well as in performance since interclass FIC matches are also improved, see [23] for research on this topic as pertaining to the human iris. Based on these results, it can be concluded that for fish iris images captured at different dates (as present in the LT dataset) rotational prealignment is required, in addition to rotation compensation in the matching stage. This finding also applies to data recorded in a realistic application, since this will result in different rotations of the iris from the same fish.

The low EERs (<4%) for the session SDs already give a first evidence that the fish iris shows a high distinctiveness, i.e., it enables to discriminate between fish in the individual sessions ($S1_{all} = 330$ fish). On the other hand, the temporal SD EERs are affected by external variations (i.e., rotational variations) and it is not possible to draw conclusions on the stability of the fish iris.

2) Rotational Prealignment and Verification Performance Analysis: The verification performances, expressed as EERs, for the different rotational prealignment strategies as well as the session- and temporal SDs enable to draw first conclusions on the stability. The results allow to determine to which degree the verification performance is affected by intrinsic changes of the fish iris and if prealignment is suited to overcome extrinsic changes, i.e., rotational variations. Also, it is not clear how the results for the session SDs, which show less rotational variations, are affected by rotational prealignment. Again, all results were computed for the semiautomated segmented fish irides to avoid side effects. Results for CNN-based segmentation enable to investigate the feasibility of a fully automated fish identification system and how it impacts the verification performances.

Results are summarized in Table I. Based on the insights of the rotation compensation analysis all EERs are computed with shifting values 16 and 32. It is not clear if a shifting value of 32 always improves the EER. Basically, a higher shifting value increases the chance to find the correct rotational alignment of two FICs from the same fish, but it also increases the risk of

TABLE I
VERIFICATION PERFORMANCES (EERS [%]) FOR THE SESSION AND TEMPORAL SDS, DIFFERENT ROTATIONAL PREALIGNMENT CONFIGURATIONS, ROTATION COMPENSATION SHIFTING VALUES 16/32 AND FOR SEMIAUTOMATED (GT) AND CNN SEGMENTED (CNN) FISH IRIDES

Segment.	Config.	Session SDs (ST)					Temporal SDs (LT)					
		$S1_{all}$	S1	S2	S3	S4	S1↔S2	S2↔S3	S3↔S4	S1↔S3	S2↔S4	S1↔S4
SHIFT 16												
GT	NO	0.65	0.71	2.52	0.15	3.91	/	/	/	/	+	-
	PCA	0.92	1.03	0.29	0.19	*	/	11.69	/	/	+	-
	MAX	3.94	0.45	0.21	0.06	*	15.52	10.32	/	15.42	29.28	-
	PCA_{ROT}	*	*	*	*	*	/	12.81	/	/	+	-
	MAX_{ROT}	*	*	*	*	*	14.96	9.87	19.6	15.96	24.44	32.56
CNN	NO	0.62	0.96	2.9	1.43	*	/	/	/	/	+	-
	PCA	0.52	0.77	1.13	1.39	4.92	/	12.73	/	/	+	-
	MAX	1.14	0.4	1.3	1.2	*	15.52	10.89	/	16.73	26.31	-
	PCA_{ROT}	*	*	*	*	*	/	12.92	/	/	+	-
	MAX_{ROT}	*	*	*	*	*	15.52	11.46	19.7	16.85	24.85	33.01
SHIFT 32												
GT	NO	0.21	0.41	0.0	0.06	1.04	/	/	/	/	+	-
	PCA	0.27	0.47	0.02	0.02	2.94	17.58	9.71	18.21	19.23	+	-
	MAX	4.11	0.48	0.01	0.05	*	15.67	9.72	/	15.83	28.84	-
	PCA_{ROT}	*	*	*	*	*	18.4	10.21	19.41	18.69	29.83	-
	MAX_{ROT}	*	*	*	*	*	14.6	10.17	17.24	15.15	23.54	34.02
CNN	NO	0.17	0.45	1.09	1.44	2.04	/	/	/	/	+	-
	PCA	0.18	0.37	1.09	1.41	1.95	17.87	11.15	19.55	/	+	-
	MAX	1.11	0.35	1.17	1.25	*	15.46	11.59	/	16.4	26.43	-
	PCA_{ROT}	*	*	*	*	*	17.65	11.79	19.65	/	+	-
	MAX_{ROT}	*	*	*	*	*	14.58	10.86	18.87	15.98	24.58	33.77

Irrelevant EERs are replaced as follows: Session SDs EERs worse than 5% are replaced by a star (∗). Green colored results signalize all EERs $< 1\%$ in the session SD results. For the first four columns in the temporal SDs EERs worse than 20% are replaced by a slash (/). For the S2↔S4 EERs results worse than 30% and for S2↔S4 EERs worse than 35% are replaced by a plus (+) and minus (−), respectively. For all temporal SDs yellow colored results highlight EERs $< 10\%$.

finding a rotational alignment of two FICs from different fish at which they are more similar to each other.

Results for GT and NO show that for the session SDs a shifting value of 16 is sufficient to achieve acceptable EERs $<4\%$, which improves to EERs $<1.04\%$ when shifting with a value of 32. As already stated, this indicates the distinctiveness of the salmon fish iris pattern. Fortunately, the EERs for the CNN results of NO (SHIFT 16 and 32) are close to the GT EERs, which indicates that the employed CNN segmentation performs well and enables to set up a fully automated system.

When considering the temporal EERs for NO (GT&CNN) two assumptions can be made: 1) as already concluded in Section IV-C1 there is more rotational variation in the temporal SDs compared to the session SDs and 2) the salmon fish iris definitely changes over time. The first assertion is shown by comparing the NO temporal SD results (GT&CNN) to all others where rotational prealignment, as well as a shift of 16, is applied. In contrast to the session SDs the EERs of the temporal SDs improve when applying rotational prealignment. This means that in case of the session SDs, which contain only little rotational variations, some of the rotational prealignment strategies add rotation to the data (EERs increase) and for the temporal SDs the majority of strategies reduce rotational variations significantly, i.e., the EERs decrease.

Results also show that for all prealignment strategies the higher shifting value 32 improves the EERs for the majority of results. Another interpretation of the results is that the current prealignment is future work and should be improved. Due to the good performance of the CNN-based segmentation most of the results are similar to the GT results. Thus, all subsequent conclusions hold for GT as well as for CNN. For the session SDs, S1, and S4 the results for SHIFT 16 and SHIFT 32 show that PCA performs better than MAX. For S2 and S3 there is no significant difference.

Contrary to the session SDs, for the temporal SDs MAX significantly outperforms PCA, especially when considering the SHIFT 16 EERs. Fig. 8(a), and (b) illustrates the cumulative MS distribution functions (CDF) for the different intraclass temporal SDs of MAX and PCA (GT), respectively. Furthermore, the interclass CDF computed over all temporal SDs (GT) is shown. The CDF of a SD gives the probability that a certain MS exists, which is less or equal to that MS. The CDFs of certain intraclass SDs and the interclass SD are used to observe their overlap and to draw conclusions about their separability. It is easy to see that compared to PCA for MAX the intraclass CDFs shift away from the interclass CDF. However, there still remains an intersection with the interclass CDF for all temporal CDFs where S4 is involved. This is also reflected by the high EERs achieved for all temporal SDs, which indicates that the salmon iris pattern changed from S3 to S4. This is further substantiated by the fact that for the session SDs and S4 with SHIFT 32 and NO (GT) an EER of 1.04% is achieved. Thus, it is very likely that the high EERs for all temporal SDs with S4 are caused by internal variations of the iris, i.e., growth of the fish eye and changing iris pattern.

Considering MAX_{ROT} and PCA_{ROT} the session SDs show that the EERs (see Table I) increase significantly compared to NO. Note that EERs worse than 5% are replaced by a star (*) in the

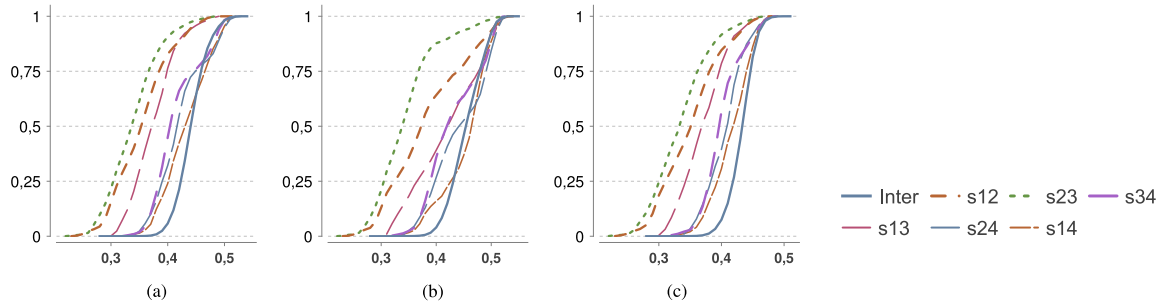

Fig. 8. Intra-/Interclass CDFs of the temporal SDs and selected rotational prealignment strategies (GT, SHIFT 16) [*X*-Axis: MS, *Y*-Axis: Cumulative Probability]. (a) MAX. (b) PCA. (c) MAX_{ROT}.

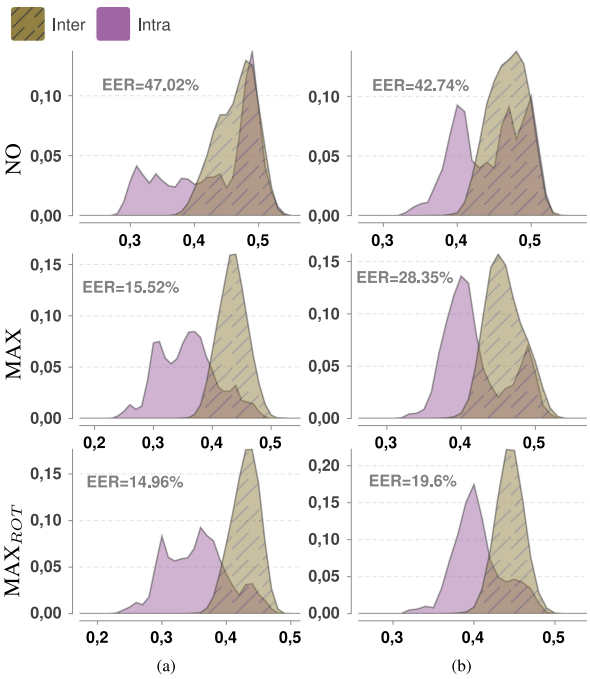

Fig. 9. Intra-/Interclass distribution charts for selected temporal SDs and selected rotational pre-alignment strategies (GT, SHIFT 16). [*X*-Axis: MS, *Y*-Axis: Probability]. (a) S1↔S2. (b) S3↔S4.

table. An explanation for this effect is that four FICs per iris and additional shifting significantly increases the risk of finding rotational alignments where the iris of different fish are similar to each other. However, the MAX_{ROT} EERs for the temporal SDs are superior to all other results. This is independent of the shifting value, confirming the assumption that if the rotational prealignment works further shift based compensation beyond what is required for a single session is not needed. Interestingly, PCA_{ROT} is not suited to improve the verification performances of the temporal SDs. The corresponding intraclass CDFs for the temporal SDs of MAX_{ROT} (GT, SHIFT 16) are shown in Fig. 8(c). Compared to the MAX CDFs in Fig. 8(a) it is obvious that the intersection of the intraclass CDFs with S4 and the interclass CDF decreases. Finally, Fig. 9 enables to compare the intraclass and interclass SDs for the temporal SDs S1↔S2 and S3↔S4 (GT, SHIFT 16) computed with NO, MAX and MAX_{ROT}. For NO the charts illustrate that rotational misalignment causes an overlap of intraclass SDs with the interclass SDs. Considering MAX this overlap is significantly reduced by rotational prealignment and rotation compensation. For MAX there still is a high overlap of the interclass and interclass SD, which is reduced when applying MAX_{ROT} for rotational prealignment.

3) Identification and Real-World Scenario Performances: By considering the identification performances for the session and temporal SDs first conclusions on the feasibility of salmon fish iris identification in a real-world scenario can be drawn. Hence, the CNN-based segmented fish irides were utilized for the identification performance experiments.

Basically, session SDs indicate the feasibility of ST identification and temporal SDs show the performance for LT identification. Identification performances are assessed based on the Rank-1 recognition rate (RR). In Figs. 10 and 11, the Rank-1 RR for the rotational prealignment strategies and the session and temporal SDs are summarized, respectively. The temporal SDs results are comparable to the verification results for SHIFT 16 and the general statements are the same. Summarized, PCA performs better than MAX and MAX_{ROT} and PCA_{ROT} improves the performance for S4 slightly. With PCA, except for S4, all Rank-1 RRs are higher than ∼98.5%. The best performance for S4 is achieved with PCA_{ROT} showing a Rank-1 RR close to ∼96%.

Results confirm that the salmon fish iris is highly distinctive and enables ST fish identification. However, same as for the verification results the identification performances for the temporal SDs again show that intrinsic variations, i.e., aging, cause decreasing Rank-1 RRs. Again, the best performances are achieved with MAX and MAX_{ROT}. The best performance is shown for the temporal SD S2↔S3 with ∼80% followed by S1↔S2 and S1↔S3. Again, this indicates that the iris changed significantly from the S3 to S4. Even S1↔S3 with ∼65% is better than ∼50% achieved for S3↔S4 with a shorter time-span between the acquisition sessions. Together with the verification performance results, it can be concluded that the robustness of fish iris biometrics suffers from a missing LT stability of the fish iris. However, the S1↔S2, S2↔S3, and S1↔S3 results indicate that identification in a real-world scenario is feasible but the system needs to consider this issue by updating the biometric templates of each fish (FIC) in short periods. Especially, at an

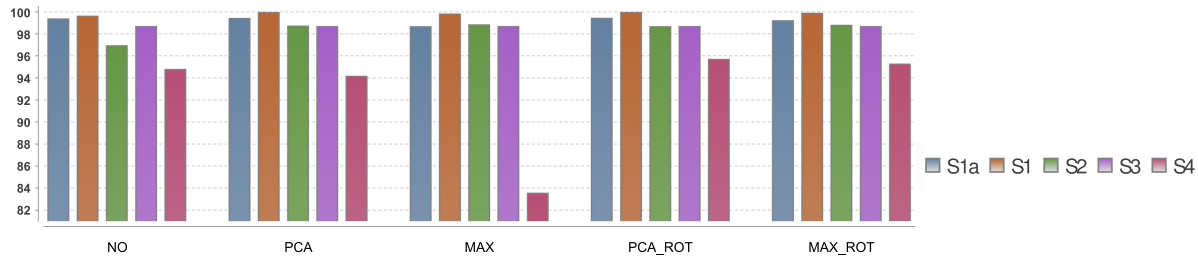

Fig. 10. Session SDs (CNN, SHIFT 16) – Identification performance evaluation [*Y*-axis: Rank-1 recognition rate (RR) %].

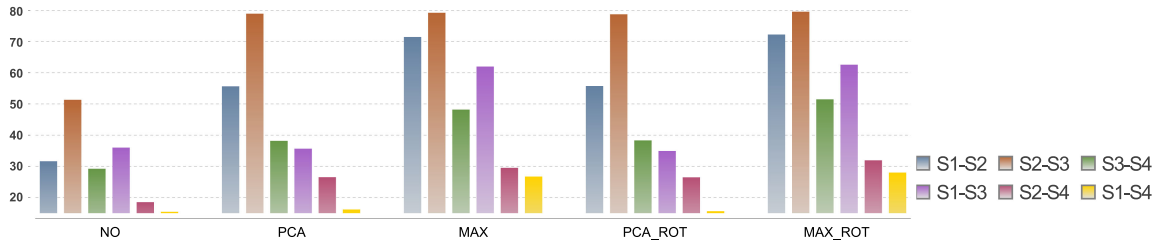

Fig. 11. Temporal SDs (CNN, SHIFT 16) – Identification performance evaluation [*Y*-axis: Rank-1 RR %].

age over 6 months this becomes crucial as the pattern changes significantly at this age.

This is also an interesting result with regard to the biometry of the human iris, since the human iris shows ageing effects, although the severity of the impact is controversial (see [24]). The fish under study have now also shown an ageing effect, which can much more readily observed and researched owing to the faster life cycle of the Atlantic salmon.

4) Comparison to Related Literature: Finally, the Atlantic fish iris identification results are compared and discussed with the literature presented in Section II. Different to the low stability of the Atlantic salmon iris, the results for Patagonian catfish in [8] showed that the lateral skin spot pattern has a high distinctiveness as well as LT stability. A direct comparison of the results is not feasible, as the approach in [8] relies on I^3S [25], which is a computer-aided photo identification application for underwater animals. With the help of this software, three reference points and all spots in each lateral image were annotated manually and the software performed the matching. If the authors achieve similar results in the future with an automated method, the approach would have great potential in terms of distinctiveness and stability.

If the skin pattern is used as a characteristic it is often not clear if it is present for all fish of the same species and if this pattern is present at all ages. The results for Atlantic salmon identification in [9], which are based on the lateral opercolum pattern indicate the nonsuitability as a biometric characteristic because some fish showed no pattern or it disappeared. Similarly, in [11], the absence of the dorsal head view pattern of Chinook salmon for a large amount of individuals has been reported.

The results presented by [12] for delta smelt identification based on dorsal head view images are comparable to ours in terms of stability. Even if the pattern was localized manually, results for automated matching indicated that the pattern changes over time and matured fish show more distinctive patterns. On the contrary, our results show that the distinctiveness of Atlantic salmon based on the iris pattern could get a little worse with older age. A comparison regarding the distinctiveness is not possible because the fish sample size was smaller and no results for one point in time (=session SDs in this article) were presented.

Compared to our session SD results the experiments for armored catfish identification using ventral images [5] and lionfish identification using lateral images [10] showed poorer recognition accuracies, although manual localization was performed.

It can be concluded, that the suitability of the skin pattern as a biometric characteristic must be examined closely, same as for the iris pattern. In the future approaches with automated skin pattern localization should be sought by the community.

The basic advantage of the iris is that most fish species show a visible iris pattern which is likely suited as a biometric characteristic to set up a FDSS. Additionally, as shown in this article the iris pattern can be localized automatically which enables automated identification.

V. Conclusion

Fish identification is a basic tool required to move from mass to smart production in intensive aquaculture. Noninvasive methods are fast, cheap, and beneficial for fish welfare. Biometric approaches based on the individuality of the skin pattern lack of visible patterns in general and missing patterns in various life phases of a single fish. Therefore, this article demonstrated the principal feasibility of Atlantic salmon fish identification using iris images as biometric characteristic. Distinctiveness and stability of the salmon fish iris were assessed based on a ST and LT dataset.

Results for 330 different fish in the ST dataset showed that the fish iris is highly distinctive. For all subsets in the ST dataset identification rates of over 95% could be achieved. The stability of the fish iris was assessed based on the LT dataset.

Due to different rotational alignments between iris images of the same fish captured at different points in time a set of rotational prealignment strategies were applied and evaluated. Experiments showed that rotation compensation in the matching stage, even with a high shifting value, is not sufficient to achieve acceptable EERs. The best results for the LT dataset were achieved with the rotational prealignment strategy MAX, which uses the maximum length pupillary CM to boundary vector for alignment. An additional improvement could be achieved by enrolling four 90° rotated templates of each iris (MAX_{ROT}), reducing errors caused by rotational prealignment resulting in at most 45° rotational error in iris images.

Results showed that the verification performances decrease with an increasing time span between the different acquisition sessions. Interestingly, results for the first two (S1↔S2 = 14.96%) and the last two successive sessions (S3↔S4 = 19.6%) sessions are worse than for the middle sessions (S2↔S3 = 9.87%). This leads to two main conclusions: 1) The salmon fish iris shows a weak stability, i.e., due to ageing (=size and pattern changes). 2) The variations caused from ageing from month 2 to 4 and 6 to 8 are much stronger than in-between from month 4 to 6.

Results achieved with semiautomated segmented fish irides were compared to those computed with a fully automated CNN-based approach. The results showed that automated segmentation is possible and comparable to that achieved with the semiautomated segmented irides. This was crucial in order to establish a fully automated fish identification system. Additionally, for a real-world scenario the identification performance of the LT dataset is of relevance and the identification rates for MAX_{ROT} on the different subsets vary between 28% and 80%. Based on the missing stability of the salmon fish iris and the accuracies for the successive subsets S1↔S2 = 72.00%, S2↔S3 = 80.00% and S3↔S4 = 51.00% the following conclusion can be made: Salmon fish iris identification is feasible in a real-world scenario with the precondition that the biometric template of each fish in the database of the biometric system is updated periodically, especially when the fish gets older than 6 months. In human biometrics this is referred to as adaptive biometric systems.

A. Future Work

It was not feasible to consider the impact and change of pigmentation with age in this article. The change in pigmentation can be disregarded for short time spans. However, given the decrease in identification performance between image acquisition sessions that are further apart in time, this may be the reason for the decrease.

Future work needs to consider a realistic environment, i.e., underwater iris images of swimming fish. For example, fish could be forced to pass through a narrative tube with their lateral side to the camera at a relatively constant distance similar to what explained in [26] and [27]. In order to compensate for differences between iris images from different sessions future experiments should consider iris image preprocessing.

Furthermore, the use of near-infrared imaging could improve the identification performance since the iris is likely pigmented given that it is an extension of the epithelial layer. It is known that the speed of adaptation and the pigmentation of the epithelial layer changes, stronger pigmentation with increasing age [15]. The impact on the pigmentation of the iris is unknown but is likely to happen. Independent of visible light or near infrared imaging, an appropriate illumination as common in human iris imaging needs to be considered. However, special care must be taken to ensure that the lighting does not pose any health risks or impacts fish welfare.

Finally, the use of other or additional biometric performance metrics should be considered in future work. The use of other metrics will depend in particular on the respective application or the focus of the investigation.

References

[1] FAO, *The State of World Fisheries and Aquaculture 2018 (SOFIA): Meeting the Sustainable Development Goals*. Food & Agriculture Organization, 2018.

[2] F. Antonucci and C. Costa, "Precision aquaculture: A short review on engineering innovations," *Aquaculture Int.*, vol. 28, pp. 1–17, 2019.

[3] M. Saberioon, A. Gholizadeh, P. Cisar, A. Pautsina, and J. Urban, "Application of machine vision systems in aquaculture with emphasis on fish: State-of-the-art and key issues," *Rev. Aquaculture*, vol. 9, no. 4, pp. 369–387, 2017.

[4] M. Sandford, G. Castillo, and T.-C. Hung, "A review of fish identification methods applied on small fish," *Rev. Aquaculture*, vol. 12, no. 2, pp. 542–554, 2020.

[5] R. Dala-Corte, J. A. Moschetta, and F. Becker, "Photo-identification as a technique for recognition of individual fish: A test with the freshwater armored catfish," *Neotropical Ichthyology*, vol. 14, 2016.

[6] J. Delcourt *et al.*, "Individual identification and marking techniques for Zebrafish," *Rev. Fish Biol. Fisheries*, vol. 28, no. 4, pp. 839–864, Sep. 2018.

[7] Y. Lu, X. He, Y. Wen, and P. Wang, "A new cow identification system based on iris analysis and recognition," *Int. J. Biometrics*, vol. 6, pp. 18–32, 2014.

[8] J. P. Barriga, J. M. Chiarello-Sosa, R. Juncos, and M. Á. Battini, "Photo-identification and the effects of tagging on the patagonian catfish hatcheria macraei," *Environ. Biol. Fishes*, vol. 98, no. 4, pp. 1163–1171, Sep. 2014.

[9] L. H. Stien *et al.*, "Consistent melanophore spot patterns allow long-term individual recognition of atlantic salmon *Salmo salar*," *J. Fish Biol.*, vol. 91, no. 6, pp. 1699–1712, Nov. 2017.

[10] L. C. T. Chaves, J. Hall, J. L. L. Feitosa, and I. M. Côté, "Photo-identification as a simple tool for studying invasive lionfish populations," *J. Fish Biol.*, vol. 88, no. 2, pp. 800–804, 2015.

[11] J. Merz, P. Skvorc, S. Sogard, C. Watry, S. Blankenship, and E. V. Nieuwenhuyse, "Onset of melanophore patterns in the head region of chinook salmon: A natural marker for the reidentification of individual fish," *North Amer. J. Fisheries Manage.*, vol. 32, no. 4, pp. 806–816, Aug. 2012.

[12] G. Castillo *et al.*, "Using natural marks to identify individual cultured adult delta smelt," *North Amer. J. Fisheries Manage.*, vol. 38, no. 3, pp. 698–705, May 2018.

[13] B. Burnside and B. Nagle, "Retinomotor movements of photoreceptors and retinal pigment epithelium: Mechanisms and regulation," *Progr. Retinal Res.*, vol. 2, pp. 67–109, 1983.

[14] F. Munz, "Vision: Visual pigments," in *Sensory Systems and Electric Organs*. San Francisco, CA, USA: Academic, 1971, vol. 5, pp. 1–32.

[15] M. A. Ali, "The ocular structure, retinomotor and photo-behavioral responses of juvenile pacific salmon," *Can. J. Zool.*, vol. 37, no. 6, pp. 965–996, 1958.

[16] L. Masek, "Recognition of human iris patterns for biometric identification," Master's thesis, Univ. Western Australia, Perth, Australia, 2003.

[17] P. W. Andreas Uhl, "Weighted adaptive hough and ellipsopolar transforms for real-time iris segmentation," in *Procs. IAPR/IEEE Int. Conf. Biometrics*, New Delhi, India, 2012, pp. 1–8.

[18] H. Hofbauer, E. Jalilian, and A. Uhl, "Exploiting superior cnn-based iris segmentation for better recognition accuracy," *Pattern Recognit. Lett.*, vol. 120, pp. 17–23, 2019.

[19] V. Badrinarayanan, A. Kendall, and R. Cipolla, "Segnet: A deep convolutional encoder-decoder architecture for image segmentation," *IEEE Trans. Pattern Anal. Mach. Intell.*, vol. 39, no. 12, pp. 2481–2495, Dec. 2017.

[20] J. Daugman, "The importance of being random: Statistical principles of iris recognition," *Pattern Recognit.*, vol. 36, no. 2, pp. 279–291, 2003.
[21] University of Salzburg, "USIT—University of Salzburg iris toolkit," 2017. [Online]. Available: http://www.wavelab.at/sources/USIT/
[22] D. Maltoni, D. Maio, A. K. Jain, and S. Prabhakar, *Handbook of Fingerprint Recognition*. New York, NY, USA: Springer, 2009.
[23] A. U. Christian Rathgeb, H. Hofbauer, and C. Busch, "Triplea: Accelerated accuracy-preserving alignment for iris-codes," in *Proc. 9th IAPR/IEEE Int. Conf. Biometrics*, 2016, pp. 1–8.
[24] H. Hofbauer, I. Tomeo-Reyes, and A. Uhl, "Isolating iris template ageing in a semi-controlled environment," in *Proc. Int. Conf. Biometrics Special Interest Group*, Darmstadt, Germany, 2016, Paper. 8.
[25] J. den Hartog and R. Reijns, "I3s: Interactive individual identification system," Accessed: Apr. 25, 2019. [Online]. Available: http://www.reijns.com/i3s/index.html
[26] J. M. Miranda and M. Romero, "A prototype to measure rainbow trout's length using image processing," *Aquacultural Eng.*, vol. 76, pp. 41–49, 2017.
[27] B. Zion, V. Alchanatis, V. Ostrovsky, A. Barki, and I. Karplus, "Real-time underwater sorting of edible fish species," *Comput. Electron. Agriculture*, vol. 56, no. 1, pp. 34–45, 2007.

Rudolf Schraml is currently working toward the Ph.D. degree with the University of Salzburg, Salzburg, Austria.

His research interests include physical object identification and authentication in different fields of applications.

Heinz Hofbauer received the doctoral degree in computer science from University of Salzburg, Salzburg, Austria, in 2013.

He works as a Researcher with the University of Salzburg, Salzburg, Austria and has published extensively in the fields of content and media security and biometrics.

Ehsaneddin Jalilian is currently working toward the Ph.D. degree with the University of Salzburg, Salzburg, Austria.

His research interests include: visual recognition, deep learning, and biometrics.

Dinara Bekkozhayeva is currently working toward the Ph.D. degree with the University of South Bohemia in České Budějovice, Czech Republic.

Her research interests are fish morphology, fish taxonomy, fish identification, and fish welfare.

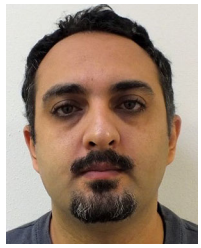

Mohammadmehdi Saberioon received the doctoral degree in precision farming engineering from Universiti Putra Malaysia, Selangor, Malaysia, in 2014.

His current research interests include applied remote sensing, field and imaging spectroscopy, and advanced artificial intelligence in different disciplines of agriculture and environmental studies.

Petr Cisar received the doctoral degree in cybernetics (visual speech recognition) from the University of West Bohemia, Pilsen, Czech Republic, in 2007.

He develops the systems and methods for fish/crayfish behavior/appearance monitoring and analysis. His research interests include application of computer vision and signal processing in the aquaculture.

Andreas Uhl received the habilitation degree in computer science and the doctoral degree in mathematics from the University of Salzburg, Salzburg, Austria, in 1996 and 2000, respectively.

He is currently a Full Professor with the Computer Sciences Department, University of Salzburg, Salzburg, Austria, where he leads the multimedia signal processing and security lab. His research interests include image and video processing, biometrics, visual data encryption, medical image analysis, and high-performance computing.